Article

Optimal Decision of Dynamic Bed Allocation and Patient Admission with Buffer Wards During an Epidemic

Chengliang Wang ![ORCID]**, Feifei Yang** *![ORCID] **and Quan-Lin Li** ![ORCID]

School of Economics and Management, Beijing University of Technology, Beijing 100124, China
* Correspondence: yangfeifei@bjut.edu.cn

Abstract: To effectively prevent patients from nosocomial cross-infection and secondary infections, buffer wards for screening infectious patients who cannot be detected due to the incubation period are established in public hospitals in addition to isolation wards and general wards. In this paper, we consider two control mechanisms for three types of wards and patients: one is the dynamic bed allocation to balance the resource utilization among isolation, buffer, and general wards; the other is to effectively control the admission of arriving patients according to the evolution process of the epidemic to reduce mortality for COVID-19, emergency, and elective patients. Taking the COVID-19 pandemic as an example, we first develop a mixed-integer programming (MIP) model to study the joint optimization problem for dynamic bed allocation and patient admission control. Then, we propose a biogeography-based optimization for dynamic bed and patient admission (BBO-DBPA) algorithm to obtain the optimal decision scheme. Furthermore, some numerical experiments are presented to discuss the optimal decision scheme and provide some sensitivity analysis. Finally, the performance of the proposed optimal policy is discussed in comparison with the other different benchmark policies. The results show that adopting the dynamic bed allocation and admission control policy could significantly reduce the total operating cost during an epidemic. The findings can give some decision support for hospital managers in avoiding nosocomial cross-infection, improving bed utilization, and overall patient survival during an epidemic.

Keywords: buffer wards; mixed-integer programming; dynamic bed allocation; patient admission control; COVID-19 pandemic

MSC: 90B50

1. Introduction

In recent years, the outbreaks of major infectious diseases have posed a significant threat to human health, life security, and economic development worldwide. For example, coronavirus disease 2019 (COVID-19) is sweeping the world rapidly, with over 500 million confirmed cases and over 6 million deaths globally reported by the World Health Organization as of 17 April 2022 (https://covid19.who.int/ (accessed on 17 April 2022)). The U.S. Department of Health and Human Services report showed that the average daily admissions peaked at 145,000 during the week in mid-January 2022 due to the impact of the Omicron variant (https://protect-public.hhs.gov/pages/hospital-utilization (accessed on 1 April 2022)). The extreme shortage of hospital beds has resulted in COVID-19 patients not being rationally scheduled and non-COVID-19 patients not receiving urgent care, which significantly increases the risk of virus transmission and patient death.

As we all know, inpatient beds are one of the critical resources in the daily operation of hospitals, and their effective dispatch directly affects the operation efficiency and service level of the whole hospital [1]. Rapid and reasonable decision-making in limited bed allocation is crucial for preventing and controlling epidemics. Hospitals must simultaneously face the following challenges: (1) First, hospitals must urgently allocate a certain number

of isolation beds at negative pressure for the treatment of COVID-19 patients. (2) Then, hospitals must guarantee necessary daily medical needs and provide essential medical services for non-COVID-19 patients with different degrees of emergency, especially those with high emergency health conditions (The U.S. Centers for Disease Control and Prevention, 2020; https://www.cdc.gov/coronavirus/2019-ncov/hcp/relief-healthcare-facilities.html (accessed on 1 April 2022)). (3) Last, to avoid cross-infection within the hospitals and to ensure the normal operation of medical facilities simultaneously, hospitals must develop relevant screening policies to screen newly arrived inpatients, especially those who have the risk of the incubation period of COVID-19 but are excluded temporarily (which we call "at-risk-of-COVID-19" patients) [2,3]. Therefore, it is an urgent problem to make a reasonable decision on bed allocation and patient admission control under limited resources during an epidemic.

At present, research on cross-infection prevention in hospitalization for infectious diseases mainly focuses on three classes: (1) Put at-risk-of-COVID-19 patients into isolation beds for separating inpatient management, for example, in Singapore and Italy [4,5]. (2) The hospitals provide each inpatient with the necessary personal protective equipment and then place them in the general wards [6]. (3) Many hospitals have set up buffer wards in emergency rooms, operating rooms, or general wards to pay close attention to new inpatients at a certain period to screen COVID-19 patients, just as in Egypt and China [3,7]. However, the first way can cause an extreme shortage of isolation beds, and in the second way, nosocomial infections may still appear despite the provision of additional personal protective equipment for inpatients. In contrast, inpatient observation in the buffer wards (a separate area for a single person in a single room) can effectively identify asymptomatic and incubated COVID-19 patients. Additionally, patients requiring acute or emergency treatment are attended to promptly in buffer wards even when nucleic acid test results are unknown, thus relieving the pressure of medical treatment for non-COVID-19 patients during a pandemic.

Our work is motivated by the need for hospital managers to rationalize bed allocation and patient admissions during the evolution of the COVID-19 pandemic so hospitals can take on the dual obligation of admitting patients and screening for latent COVID-19 patients to prevent cross-infection and improve overall patient survival. At the same time, hospital administrators face the challenge of balancing limited resources in different types of wards and patients caused by the time-varying nature and high uncertainty of hospital resource requirements. In this paper, we study the problem of dynamic bed allocation and patient admission control in a hospital with three types of wards in the COVID-19 epidemic. The bed manager faces trade-offs: (1) From the perspective of dynamic bed allocation, the arrival rate of COVID-19 patients directly leads the isolation beds to be insufficient or empty due to the fluctuations of the epidemic. In this context, balancing the allocation of beds among different types of wards is critical to improving bed utilization. (2) From the perspective of patient admission control, admitting too many elective patients will delay the treatment of emergency and COVID-19 patients in the future while admitting too few elective patients may result in a waste of medical resources. To solve the above problems, we propose an MIP model to jointly optimize bed resource allocation and patient admission. Specifically, the bed manager should make the bed allocation decisions on the isolation, buffer, and general wards and how many elective patients should be admitted in each period. Considering the stochastic arrivals, the uncertainty of the length of stay, and the preference of hospital administrators, we propose a dynamic bed allocation and patient admission control problem with the objective of minimizing the total operating cost reflecting multiple criteria. The total operating cost is composed of the bed retrofitting cost, the empty cost, the waiting cost, the rejection cost, and the delayed transfer cost.

Based on the above analysis, the main contributions to this study are:

(1) Considering buffer wards established to prevent cross-infection and secondary infection of COVID-19 inside the hospital, we study the dynamic bed allocation and patient admission control problem with three different types of wards during an epidemic, isolation

wards for admission of COVID-19 patients, buffer wards to screen the incubation risk of COVID-19, and general wards to admit emergency and elective patients who have excluded the risk of the incubation period of COVID-19.

(2) We formulate a MIP model that considers three different types of wards and patients for dynamic joint optimization of bed allocation and patient admission decisions. In addition, we propose a BBO-DBPA algorithm to solve this joint optimization problem and obtain an optimal decision scheme that minimizes the total operating cost of the hospital.

(3) Numerical experiments are conducted to investigate how the optimal decision scheme depends on some key parameters. Furthermore, we evaluate the performance of the optimal decision scheme by comparing it with some benchmark policies which are executable and have significant practical implications.

The remainder of this paper is organized as follows. In Section 2, we briefly review the relevant literature. Section 3 presents the problem description and symbol introduction. Section 4 gives the basic optimization formula for the programming problems. Section 5 describes the proposed BBO-DBPA algorithm. In Section 6, we analyze the numerical results and evaluate the performance of the optimal policy with benchmark policies. Section 7 makes conclusions and presents future research.

2. Literature Review

This paper focuses on the impact of dynamic bed allocation and patient admission control policies during the COVID-19 pandemic. So, the following three streams of literature contribute to this research: the inpatient management of epidemics, bed planning, and patient admission scheduling.

For the inpatient management of epidemics, hospitals tend to adopt three ways of admission to arrange newly arrived patients during the pandemic. The first is to place both confirmed, and unconfirmed patients in isolation wards [5,8]. Heins et al. [9] forecasted the short-term bed occupancy of patients with confirmed and suspected COVID-19 by Monte Carlo simulation and used the predictions to guide bed allocation. The second way for hospitals is to admit patients who cannot be confirmed for COVID-19 to the general wards with additional personal protection [6]. A cross-sectional study by Liu et al. [10] found that this could somewhat free up isolation beds. Unfortunately, unexpected infections still occur. In order to prevent and control the epidemic more strictly, the last method is to set up buffer wards to provide timely treatment to critically ill patients in some hospitals [3,7,11,12]. In terms of the operation management of hospitals with buffer wards during a pandemic, Liu et al. [13] built the infinite- and finite-horizon Markov decision process (MDP) models and proposed various iteration algorithms to obtain the optimal policy.

The bed planning problem concerns how many beds should be allocated among multiple patient classes. From the perspective of bed types, scholars have studied single and multiple types of beds. For the single type of beds, some researchers have focused on solving different specific problems and developed integer programming models. Pishnamazzadeh et al. [14] studied the bed planning problem by considering elastic management, developed an integer planning model and solved it using a simulated annealing algorithm. Lei et al. [15] considered the bed planning problem for both deterministic and stochastic length of stay and constructed an integer planning model by solving it using the CPLEX solver. Research on the multi-type bed planning problem mainly focuses on two classes: how to assign beds with specific features to a set of patients with specific requirements and how many beds are configured in the various departments considering different goals. Most papers construct integer programming models for the first class and solve them using heuristic algorithms [16,17]. For the second class, Mathematical programming models and simulation models are the most commonly used methods to deal with this problem [18–21]. In terms of dynamic bed management in a pandemic, Ma et al. [22] developed a dynamic programming model to study the allocation of two types of beds (isolation beds and ordinary beds) and the effect of the subsidy policy on serving three types of patients (COVID-19,

emergency, and elective patients). The study shows that the dynamic allocation between isolation and ordinary beds can provide better utilization of bed resources.

The patient admission scheduling problem (PAS problem) is first studied by Demeester et al. [23]. It refers to assigning patients to appropriate beds within the planning horizon to maximize treatment efficiency, patient comfort, and medical resource utilization while considering patients' preferences and meeting necessary medical restrictions. From a strategic point of view, patient admission scheduling is a kind of resource planning. To solve this kind of problem, scholars have built integer programming optimization models and put forward effective search algorithms to solve the specific problem. Relevant studies can be divided into two streams according to whether the research needs are random or not. Some scholars have studied the needs of deterministic patients and constructed integer programming models, which have solved these models using a tabu search algorithm [24], general low-level heuristics algorithm [25], column generation algorithm [26], biogeography-based optimization algorithm [27,28], Fix-and-Relax and fix-and-optimization method [29], exact solution method [30] and so on. Another kind of literature has studied the dynamic situation of the PAS problem, that is, the patient demand is random. They built the integer programming models and solved them by using the simulated annealing algorithm [31], late acceptance hill-climbing algorithm [32], and column generation algorithm [33].

Although the current research on optimizing bed allocation and patient admission control has achieved initial results, it still faces challenges. In terms of the research on bed allocation decisions, most researchers have studied the problems of hospital bed configuration in different departments [34,35]. Specifically, Broek d'Obrenan et al. [36] considered the bed allocation for multi-types of patient flow among different departments. However, the above study only considered the allocation of hospital beds for ordinary patients and ignored the allocation of isolation beds for infectious patients during the COVID-19 pandemic. Studies on patient admission scheduling have considered the problem that different types of patients are assigned to different types of wards according to their preferences [22,30]. However, few studies consider bed retrofitting between different types of wards. For the optimal decision under the pandemic, some papers noted the optimization of inpatient admission only in buffer wards (e.g., Liu et al. [13]) but did not consider the reality that different types of patient flows need to be placed in different types of wards. To our knowledge, almost no one has studied the dynamic bed allocation and patient admission control problem considering the buffer wards during the pandemic. In this study, we study the dynamic bed allocation and patient admission control problem in a hospital with three different types of wards during an epidemic. Furthermore, we propose a mix-integer programming approach to obtain optimal dynamic bed allocation and patient admission control policies.

3. Problem Statement

In this section, we describe the problem of dynamic bed allocation and patient admission control, considering three different types of wards in a hospital during a pandemic. Additionally, we present the system structure and mathematical notations.

3.1. Problem Description

To illustrate our problem more clearly, Figure 1 illustrates this problem of dynamic bed allocation and patient admission decisions for one hospital. Inpatients are divided into three types after the initial screening at the triage table: confirmed COVID-19 patients, at-risk-of-COVID-19 emergency patients, and at-risk-of-COVID-19 elective patients. To ease analysis, patients with positive COVID-19 nucleic acid we considered are unvaccinated and are infected for the first time. Additionally, at-risk-of-COVID-19 patients refer to those who have not confirmed COVID-19 temporarily but have the incubation risk of COVID-19. For simplicity, we define these three types of patients as COVID-19, emergency, and elective patients in the remainder of the paper. During the regular management of the COVID-19 epidemic, the hospital has three types of wards: isolation wards, buffer wards, and general

wards. If there are empty beds in the isolation wards, COVID-19 patients are admitted and occupy an empty bed directly upon arrival. As introduced above, emergency and elective patients should be sent to the buffer wards for COVID-19 screening. Similar to COVID-19 patients, emergency patients are directly admitted once they arrive. Unlike the first two, the bed managers perform admission control for elective patients: admit them to the buffer wards directly or let them join the waiting queue. In the buffer wards, once an inpatient has been diagnosed with COVID-19, this patient should be immediately moved to the isolation wards; otherwise, the patient will be excluded from COVID-19 risk and discharged or transferred to the general wards. The maximum duration of patient observation in the buffer wards is usually between 3 and 6 days. To make reasonable and efficient use of bed resources, hospitals adopt a dynamic bed allocation policy, that is, retrofitting some empty beds in one type of ward into beds in other types of wards. Note that the number of empty beds reserved in different types of wards differs at the beginning of the planning horizon. Based on the process described above, bed managers need to decide the number of retrofitted beds among different types of wards and the number of elective patients admitted to buffer wards in each planning period.
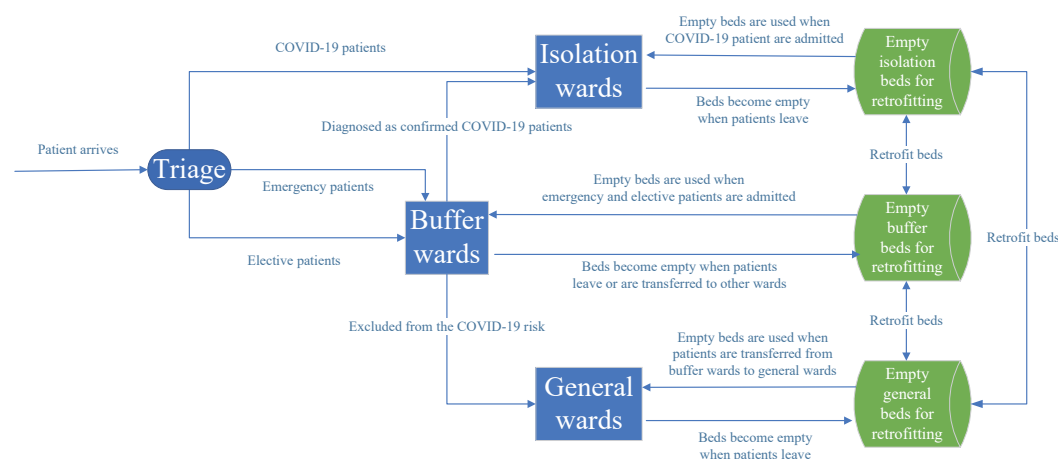

Figure 1. The illustration of patient flow and bed allocation considering buffer wards.

According to the epidemiological characteristics, the epidemic shows a fluctuating trend. To cover the entire epidemic trend, we assume that the arrival process of COVID-19 patients shows the characteristics of first increasing and then decreasing. Additionally, we assume that inpatients are not allowed direct access to the general wards during an epidemic to prevent nosocomial infections, which is in line with the literature, for example, He et al. [7]. For ease of understanding, we give the sequence of events in any period as follows.

1. At the beginning of period t, the hospital manager ascertains the number of beds occupied by different types of patients and the total number of beds in each type of ward, respectively. In addition, the number of elective patients in the waiting queue is obtained.
2. The hospital manager retrofits some beds in each type of ward.
3. Patients in buffer wards are transferred to isolation wards or general wards. The hospital manager obtains the number of patients requiring to be transferred and actually transferred from buffer wards to other types of wards according to the bed information of the wards, respectively.
4. Newly arrived patients are admitted. The COVID-19 patients must be admitted immediately using the reserved empty isolation beds. Additionally, the hospital should admit emergency patients upon arrival to the buffer wards due to the greater urgency level than elective patients. Moreover, new incoming elective patients join

the waiting list if they are not admitted. Elective patients who cannot be admitted in this period will be evaluated as to whether they will be admitted in the later periods.

5. At the end of period t, the cured patients are discharged from the designated inpatient wards. At the same time, empty beds are cleaned following cleaning and disinfecting procedures before admitting new patients or retrofitting other types of wards. This is a common setting in the literature, e.g., Liu et al. [13] and Ma et al. [22].

3.2. Definition of Parameters and Variables

We introduce a summary of the notations defined and additional parameters and variables in Table 1. Note that, for notational and model simplicity, the bed retrofit between the general and isolation beds can be carried out with the intermediate medium of buffer beds.

Table 1. Notations of the model.

Sets	Definitions
I	The set of patient types, indexed by i. $i \in I = \{1, 2, 3\}$, where type 1, type 2, and type 3 represent the COVID-19 patients, the emergency patients, and elective patients, respectively
J	The set of ward types, indexed by j. $j \in J = \{1, 2, 3\}$, where type 1, type 2, and type 3 denote the isolation wards, buffer wards, and general wards, respectively
L	The set of bed retrofit policies, indexed by l. The bed retrofit policies includes four types: $l = 1$ represents the retrofit from buffer beds to isolation beds and $l = 3$ for reverse conversion; $l = 2$ represents the retrofit from general beds to buffer beds and $l = 4$ for reverse conversion
T	The set of time periods, indexed by t

Parameters	Definitions
N	The total number of beds in the hospital
$\lambda_{i,j,t}$	The number of patient arrivals in type $i \in I$ in ward type $j \in J$ in period $t \in T$
$d_{i,j,t}$	The number of type $i \in I$ patients who need to transfer from buffer wards to ward type $j \in J$ in period $t \in T$
$\mu_{i,j,t}$	The number of patients' discharge in type $i \in I$ in ward type $j \in J$ in period $t \in T$
c_l	The unit retrofitting cost of adopting the bed retrofit policy $l \in L$
δ_j	The opportunity cost of an empty bed in ward type $j \in J$
σ	The waiting cost of an elective patient in the waiting queue per unit time
h_i	The rejection cost of a type $i \in I$ patient
$\sigma_{i,j}$	The delaying cost of a type $i \in I$ patient that needs to be transferred but is delayed

Variables	Definitions
$n_{l,t}$	The number of beds retrofitted by policies $l \in L$ in period $t \in T$
x_t	The number of elective patients admitted to the buffer wards in period $t \in T$
$X_{i,j,t}$	The number of inpatients in type $i \in I$ in ward type $j \in J$ in period $t \in T + 1$
$Y_{j,t}$	The number of beds in ward type $j \in J$ in period $t \in T + 1$, including occupied and empty beds
$D_{i,j,t}$	The number of patients in type $i \in I$ transferred from the buffer wards to ward type $j \in J$ in period $t \in T$
W_t	The number of patients in the waiting queue in period $t \in T + 1$ (i.e., the length of waiting queue)

4. Mathematical Formulation

In this section, we consider a finite planning horizon of T periods and give a mathematical formulation of the dynamic bed allocation and patient admission control problem by developing a MIP model. The objective of our problem is to minimize the total operating cost, including the bed retrofitting cost, the empty cost, the waiting cost of elective patients, the rejection cost of COVID-19 patients and emergency patients, and the delayed transfer

cost of patients who should be transferred but were not. The decision variables are $n_{i,t}$ and x_t. Based on the above analysis, this problem can be formulated as follows:

$$\min \ Z = \sum_{t \in T} \sum_{l \in L} n_{l,t} c_l + \sum_{t \in T} w W_t + \sum_{t \in T} \sum_{j \in J} \delta_j (Y_{j,t+1} - \sum_{i \in I}(X_{i,j,t+1} + \mu_{i,j,t})) +$$

$$\sum_{t \in T} \sum_{j \in J} \sum_{i \in I} \sigma_{i,j}(d_{i,j,t} - D_{i,j,t}) + \sum_{t \in T} h_1 [\lambda_{1,1,t} - (Y_{1,t+1} - \sum_{i \in I} X_{i,1,t} - \tag{1}$$

$$\sum_{i \in I} D_{i,1,t})] + h_2 [\lambda_{2,1,t} - (Y_{2,t+1} - \sum_{i \in I} X_{i,2,t} + \sum_{j \in J} \sum_{i \in I} D_{i,1,t})]$$

Subject to

$$n_{1,t} \le Y_{2,t} - \sum_{i \in I} X_{i,2,t} \quad \forall t \in T \tag{2}$$

$$n_{2,t} \le Y_{3,t} - \sum_{i \in I} X_{i,3,t} \quad \forall t \in T \tag{3}$$

$$n_{3,t} \le Y_{1,t} - \sum_{i \in I} X_{i,1,t} \quad \forall t \in T \tag{4}$$

$$n_{4,t} \le Y_{2,t} - \sum_{i \in I} X_{i,2,t} - n_{1,t} \quad \forall t \in T \tag{5}$$

$$n_{1,t} n_{3,t} = 0 \quad \forall t \in T \tag{6}$$

$$n_{2,t} n_{4,t} = 0 \quad \forall t \in T \tag{7}$$

$$Y_{1,t+1} = Y_{1,t} + n_{1,t} - n_{3,t} \quad \forall t \in T \tag{8}$$

$$Y_{2,t+1} = Y_{2,t} + n_{2,t} + n_{3,t} - n_{1,t} - n_{4,t} \quad \forall t \in T \tag{9}$$

$$Y_{3,t+1} = Y_{3,t} + n_{4,t} - n_{2,t} \quad \forall t \in T \tag{10}$$

$$D_{2,j,t} = \min\{Y_{j,t+1} - \sum_{i \in I} X_{i,j,t}, d_{2,j,t}\} \quad \forall j \in J, \forall t \in T \tag{11}$$

$$D_{3,j,t} = \min\{Y_{j,t+1} - \sum_{i \in I} X_{i,j,t} - D_{2,j,t}, d_{3,j,t}\} \quad \forall j \in J, \forall t \in T \tag{12}$$

$$x_t \le \lambda_{3,2,t} + W_t \quad \forall t \in T \tag{13}$$

$$x_t \le \max\{Y_{2,t+1} - \sum_{i \in I} X_{i,2,t} + \sum_{i \in I} D_{i,1,t} + \sum_{i \in I} D_{i,3,t} - \lambda_{2,2,t}, 0\} \quad \forall t \in T \tag{14}$$

$$X_{i,1,t+1} = X_{i,1,t} + D_{i,1,t} + \min\{\lambda_{i,1,t}, Y_{1,t+1} - \sum_{i \in I}(X_{i,1,t} + D_{i,1,t})\} -$$

$$\mu_{i,1,t} \quad \forall t \in T \tag{15}$$

$$X_{2,2,t+1} = X_{2,2,t} - D_{2,1,t} - D_{2,3,t} + \min\{\lambda_{2,2,t}, Y_{2,t+1} -$$

$$\sum_{i \in I}(X_{i,2,t} - D_{i,1,t} - D_{i,3,t})\} - \mu_{2,2,t} \quad \forall t \in T \tag{16}$$

$$X_{3,2,t+1} = X_{3,2,t} - D_{3,1,t} - D_{3,3,t} + x_t - \mu_{3,2,t} \quad \forall t \in T \tag{17}$$

$$W_{t+1} = W_t + \lambda_{3,2,t} - x_t \quad \forall t \in T \tag{18}$$

$$X_{i,3,t+1} = X_{i,3,t} + D_{i,3,t} - \mu_{i,3,t} \quad \forall i \in I, \forall t \in T \tag{19}$$

Equation (1) is the objective function by minimizing hospital operating costs, including five parts. The first term refers to the bed retrofitting cost. The second term is associated with the waiting cost. The third term indicates the empty cost of the bed, where $\sum_{i \in I}(X_{i,j,t+1} + \mu_{i,j,t})$ represents the maximum number of patients before discharge in wards j at period t. The fourth term represents the delayed transfer cost. The last two items express the rejection costs of COVID-19 patients and emergency patients, where $Y_{1,t+1} - \sum_{i \in I} X_{i,1,t} - \sum_{i \in I} D_{i,1,t}$

represents the number of beds that can receive COVID-19 patients, and $Y_{2,t+1} - \sum\limits_{i \in I} X_{i,2,t} + \sum\limits_{j \in J} \sum\limits_{i \in I} D_{i,1,t}$ represents the number of beds that can receive emergency patients.

Constraints (2)–(5) ensure that the number of retrofitted beds is no more than the number of empty beds in different types of wards. Note that the empty beds in the buffer wards should be the first ones retrofitted to isolation beds and then the general beds, considering the pandemic control. Constraints (6) and (7) guarantee that no bed is repeatedly retrofitted between any two types of beds in any period t. Constraints (8)–(10) are bed conservation. Constraints (11)–(12) represent the patient transfer relationship, where $Y_{j,t+1} - \sum\limits_{i \in I} X_{i,j,t}$ and $Y_{j,t+1} - \sum\limits_{i \in I} X_{i,j,t} - D_{2,j,t}$ show the number of empty beds in type 2 and type 3 wards before the patients were transferred, respectively. Constraint (13) ensures that the number of elective patients admitted to buffer wards does not exceed the sum of newly arrived patients and patients waiting in the queue in period t. Constraint (14) ensures that the number of elective patients admitted is no more than the number of empty beds in the buffer wards after admitting emergency patients. Constraints (15)–(19) are the patient flow conservation where a and b represent the number of empty beds before patients are admitted to type 1 and type 2 wards, respectively.

5. The Solution Method

In this section, we propose a BBO-DBPA algorithm to solve the dynamic bed allocation and patient admission control problem. Biogeography-based optimization (BBO) is a new effective evolutionary algorithm that is often used for solving NP-hard problems, and it is proven to have a better performance compared to some other evolutionary algorithms [37]. To ensure that all solutions in the operation of the BBO-DBPA algorithm meet the model constraints, we first provide the solution representation in the following.

5.1. Solution Representation and Decoding

In this research, we consider some constraints when representing the solutions so that the solutions will always be feasible in the following optimization operations. In order to represent all decision variables conveniently, we present each feasible solution in a three-part vector. The first part, $rd\_n_{1,3,t}$, shows the retrofitting between buffer wards and isolation wards. The second part, $rd\_n_{2,4,t}$, represents the retrofitting between buffer wards and general wards. The third part, rd_x_t, indicates the number of elective patients admitted. These three parts have T cells, and each cell is a real number between 0 and 1.

Equations (20) and (21) describe the decoding process for $rd\_n_{a,a+2,t}$, $a = 1, 2$.

$$tmp_{a,t} = \lceil rd\_n_{a,a+2,t}(freebed_{a,t} + freebed_{a+1,t}) - 0.5 \rceil - freebed_{a+1,t} \tag{20}$$

$$\begin{cases} n_{a,t} = -tmp_{a,t} & \text{if } tmp_{a,t} < 0 \\ n_{a+2,t} = tmp_{a,t} & \text{if } tmp_{a,t} \geq 0 \end{cases} \tag{21}$$

where $tmp_{a,t}$ is an intermediate variable, $freebed_{j,t}$ represents the number of empty beds in wards j in period t, and

$$freebed_{j,t} = Y_{j,t} - \sum\limits_{i \in I} X_{i,j,t} \tag{22}$$

Equation (23) describes the decoding process rd_x_t.

$$x_t = \begin{cases} rd\_x_t(freebed_{2,t} - \lambda_{2,2,t}) & \text{if } 0 \leq freebed_{2,t} - \lambda_{2,2,t}) < \lambda_{3,2,t} + W_t \\ rd\_x_t(\lambda_{3,2,t} + W_t) & \text{if } \lambda_{3,2,t} + W_t \leq freebed_{2,t} - \lambda_{2,2,t}) \end{cases} \tag{23}$$

This solution representation method can ensure that the solution in the optimization operation always meets constraints (2)–(7) and (13)–(14).

5.2. Creating Initial Solutions

In the BBO-DBPA algorithm, the diversity of initially generated solutions can significantly affect the effectiveness of the optimization process. We use generating solutions twice to increase the diversity of the initial generation solutions. In the first step, some solutions are randomly generated. In the second step, if there are duplicates among these solutions, this number of solutions is randomly generated to replace these duplicates. This operation ensures that the generated solutions are likely to be different.

5.3. Migration

The BBO-DBPA algorithm uses migration operation to share the features from good solutions to poor solutions effectively. The migration operation can preserve good solutions and further expand the search scope of the solutions. Each solution will be migrated in the algorithm based on the value of the immigration rate ($\lambda(s)$) and the emigration rate (μ_s), which is calculated as in Equations (24) and (25), respectively. According to (24) and (25), the good solution has a larger emigration rate and a lower immigration rate than the poor solution.

$$\lambda(s) = I(1 - \text{HSI}_s / \text{HSI}_{\max}), \tag{24}$$

$$\mu(s) = E\text{HSI}_s / \text{HSI}_{\max}, \tag{25}$$

where I is the maximum immigration rate; E is the maximum emigration rate; HSI_s is the fitness value of solution s. The better the solution, the smaller the total cost and the larger the fitness value. $\text{HSI}_{\max}$ is the maximum fitness value. Algorithm 1 shows the migration operation of the BBO-DBPA algorithm.

Algorithm 1 The pseudo-code of the migration operation.

1: $s \Leftarrow$ the solution s
2: length $(s) \Leftarrow$ the size of the solution
3: $\lambda(s) \Leftarrow$ calculate the migration rate of all solutions according to Equation (24)
4: $\mu(s) \Leftarrow$ calculate the migration rate of all solutions according to Equation (25)
5: **For** i from 1 to length(s) **do**
6: $\quad$ NOC $\Leftarrow$ the number of codes, the value of NOC is $3T$
7: $\quad$ **For** j from 1 to NOC **do**
8: $\quad\quad$ $r_1 \Leftarrow$ random value between 0 and I
9: $\quad\quad$ **If** $r_1 < \lambda(s)$ **then**
10: $\quad\quad\quad$ $s_k \Leftarrow$ random solution with a probability proportional to $\mu(s)$
11: $\quad\quad\quad$ $s_i(j) = s_k(j)$
12: $\quad\quad$ **End if**
13: $\quad$ **End for**
14: **End for**

5.4. Mutation

In the BBO-DBPA algorithm, a mutation operation is performed to increase the variety of solutions and to escape from the local optimality trap. Different solutions have different mutation rates. The mutation rate of the solution s is related to the prior probability of existence s (P_s). In general, high and low HSI solutions are less likely to exist than medium HSI solutions. The relationship between P_s and HSI is shown in Figure 2.

The mutation rate $m(s)$ is calculated as in Equation (26).

$$m(s) = m_{\max}(1 - P_s / P_{s_k}), \tag{26}$$

where $m_{\max}$ is the maximum mutation probability; P_{s_k} is the maximum prior probability of existence.

If only the mutation operation described above is performed, the mutation probability of the good solutions and the poor solutions is relatively large. This way allows the poor solutions to improve but also makes the good solutions likely to worsen. To keep the good

solutions, we add the elite strategy to the mutation operation of the BBO-DBPA algorithm. We only perform the mutation operation on the poor half of all solutions. Algorithm 2 shows the mutation operation of the BBO-DBPA algorithm.
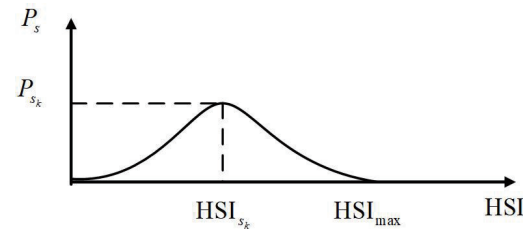

Figure 2. The relationship between P_s and HSI.

Algorithm 2 The pseudo-code of the migration operation.

1:   $s \Leftarrow$ the solution s
2: **For** i from 1 to length(s)/2 **do**
3:      $m(s) \Leftarrow$ the mutation probability of solution s
4:      **For** j from 1 to NOC **do**
5:          $r_2 \Leftarrow$ random value between 0 and E
6:          **If** $r_2 < m(s)$ **then**
7:             $s_i(j) = s_i'(j)$random solution with a probability proportional
8:             to $\mu(s)$
9:          **End if**
10:     **End for**
11: **End for**

5.5. The Structure of the BBO-DBPA Algorithm

The general framework of the BBO-DBPA algorithm is shown in Figure 3. Specifically, the experiment is conducted in the following steps:

Step 1: Setting the parameters of the algorithm, including the maximum number of iterations (maxGeneration), the size of the initially generated solutions (N), the maximum immigration rate (I), the maximum emigration rate (E), and the maximum prior probability of existence (P_{s_k}), the maximum mutation probability (m_{max}).

Step 2: Initiating solutions. The BBO-DBPA algorithm generates the initial solutions as described in Section 5.2 and starts the improvement loop after generating the initial solutions.

Step 3: Sorting of solutions. The costs of the decision options represented by those solutions are calculated as described in Section 5.1, and the fitness values are given to these solutions. Based on it, all solutions are sorted from largest to smallest.

Step 4: Migration operation. Execute the migration operation as described in Section 5.3.

Step 5: Mutation operation. Execute the mutation operation as described in Section 5.4.

Step 6: If the number of iterations is greater than maxGeneration, stop the iteration and output the optimal solution; otherwise, proceed to Step 3.
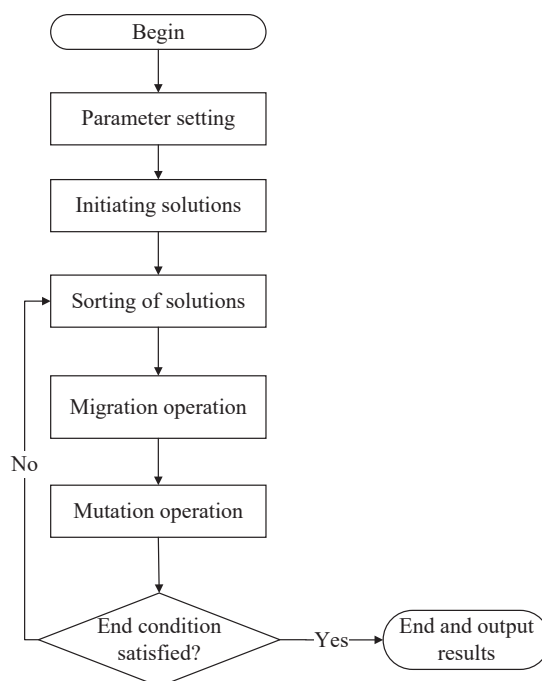
Figure 3. The flow chart of the BBO-DBPA algorithm.

6. Computational Experiments

In this section, we first analyze the base case by implementing the BBO-DBPA algorithm with a large finite iteration to find the optimal policy. Then, we present a sensitivity analysis to discuss how the optimal policy depends on some key parameters. Finally, the performance advantages are examined by comparison with some benchmark policies. All the experiments are performed in MATLAB R2019b software. The experiments were run on a computer with Windows 10 and an Intel Core i5-11400H processor with a 2.70 GHz frequency and 16 GB of RAM.

6.1. Data Setting

The main data source is obtained from the public data website, which provides relevant hospitalization data for the benchmark example in Demeester et al. [24] (https://people.cs.kuleuven.be/wim.vancroonenburg/pas/, accessed on 17 April 2022). Specifically, we set N = 286, T = 14, $X_{2,3,1}$ = 15, $X_{3,3,1}$ = 168. In addition, the information on arrival and discharge for ED and elective patients is given in Appendix A1. Because there is no benchmark dataset available for the problem formulated in this study, we refer to the real data of reported COVID-19 from March 1 to March 7 and 27 April to 3 May 2022, in Jilin province in China. It has raised the government's concerns due to the sudden outbreak of the regional epidemic (please see Appendix A2 for specific data). This number of reported COVID-19 was chosen as a benchmark for simulating the volatility of the pandemic and effectively operating our proposed model at a given scale (i.e., 286 total beds). According to Pollock and Lancaster [38], for the patient transfer in the buffer wards, we consider that 80% of the number of reported COVID-19 (as type i = 1 patient) enter the isolation wards directly, and 20% of the number of reported COVID-19 (as type i = 2 or 3 patients) enter the buffer wards to spend the observation period. We assume that COVID-19 patients in the incubation period will be detected during the observation period in the buffer wards. Thus, we set the observation period as three days based on COVID-19 evolution characteristics [39,40]. The computer randomly generates the detection time of confirmed COVID-19 patients in the buffer wards. In addition, the computer randomly generates the discharge times based on the average length of stay of 7 days for COVID-19 patients [41]. To ease understanding, we show all the hospitalization information of the three types of patients in the base case

in Appendix A3. Based on Ma et al. [22] and communication with medical staff in real hospitals, we set the unit retrofitting cost: $c_l = 10$ for $\forall l \in L$; the opportunity cost of an empty bed: $\delta_1 = 3$; $\delta_2 = \delta_3 = 2$; the waiting cost of an elective patient in the waiting queue per unit time: $w = 11$; the rejection cost: $h_1 = 500$, $h_2 = 150$, $h_3 = 0$; and the delaying cost of a type-i patient that requires to be transferred but is delayed: $\sigma_{i,j} = 1$, $\forall i \in I$, $\forall j \in I$.

Furthermore, we modify the values of some parameters to investigate their impact on the sensitivity analysis. Table 2 shows the sensitivity analysis numerical cases we considered. About the parameters of the BBO-DBPA algorithm, we set the number of initial solutions at 2000, the number of iterations at 150, the maximum immigration rate at 1, the maximum emigration rate at 1, and the maximum mutation rate at 0.02.

Table 2. Information on sensitivity analysis of numerical cases.

Case	Modified Parameter	Values
1	The total number of beds (N)	206, 246, **286** [1], 326, 366
2	The number of COVID-19 patients' arrival ($\lambda_{1,1,t}$)	Multiple 0.5, 0.75, **1**, 1.25, 1.5 of base case's arrival rate of COVID-19 patients
3	The number of COVID-19 patients' arrival ($\lambda_{3,2,t}$)	Multiple 0.8, 0.9, **1**, 1.1, and 1.2 of base case's arrival rate of elective patients

[1] The bolded numbers are the same as the values in the base case.

6.2. Base Case Study

We use the BBO-DBPA algorithm with a large finite space. After 992 s of running time and 150 iterations, we obtain the optimal policy with the minimum total operating cost of 22,672 in this hospital system. We present the results in Table 3. The results show that the number of buffer beds retrofitted to isolation beds first increases and then decreases. That is because the demand for isolation beds increases as more and more new COVID-19 patients arrive, then decreases in the planning horizon. Intuitively, there is no retrofit of buffer beds to general beds because the demand for isolation beds is higher than that for buffer beds or general beds during the pandemic.

Table 3. Hospital optimal decision scheme for dynamic bed allocation and admission control.

Decision	$t=1$	$t=2$	$t=3$	$t=4$	$t=5$	$t=6$	$t=7$	$t=8$	$t=9$	$t=10$	$t=11$	$t=12$	$t=13$	$t=14$
$n_{1,t}$	4	0	13	20	14	35	46	48	35	15	15	13	2	0
$n_{2,t}$	56	51	53	12	11	7	0	22	19	29	2	3	0	2
$n_{3,t}$	0	1	0	0	0	0	0	0	0	0	0	0	3	0
$n_{4,t}$	0	0	0	0	0	0	0	0	0	0	0	0	0	0
x_t	60	51	50	25	28	20	8	8	20	28	15	6	9	11

The number of general beds retrofitted to buffer beds shows two peaks respectively on days 1–3 and days 8–10, and the number is higher during days 1–3 than days 8–10. That is because buffer beds are in short supply when faced with a demand from non-COVID-19 patients in the early periods. After the incubation period (3 days), the number of general beds retrofitted to buffer beds decreases to ensure the needs of the general wards as patients in the buffer wards start to move to the general wards. The reason for the peak on days 8–10 is that the decrease in the number of patients admitted to the buffer wards on days 4–7 leads to the decrease in the number of patients transferred to the general wards on days 8–10, which leads to more empty beds to retrofit. In addition, three isolation beds are retrofitted to buffer beds on day 13. The reason is that with fewer COVID-19 patients arriving in the latter periods, the empty isolation beds can be retrofitted into buffer beds to admit more non-COVID-19 patients.

Figures 4 and 5 give the total number of beds in different types of wards and the number of patients in the waiting queue. In Figure 4, the blue line indicates the number of beds in the isolation wards, the red line represents the number of beds in the buffer wards,

and the green line shows the number of beds in the general wards. Figure 4 shows that the number of isolation beds increases rapidly in the first seven days, then the increasing trends are moderate in the latter periods. Moreover, the number of buffer beds increases rapidly from day 1 to 4 and decreases gradually after day 5. Furthermore, the number of general beds shows an overall downward trend. The reason for the above trend corresponds to the decision variables, which are shown in Table 3. Figure 5 shows that the number of patients in the waiting queue gradually increases over time. Intuitively, as the number of COVID-19 arrivals increases, some buffer beds are retrofitted to isolation beds, the buffer beds are in short supply, and more and more elective patients are joining the waiting queue to wait for inpatient services. The optimized results can provide decision support for hospital administrators. During a pandemic, hospitals should make some beds empty to admit future arrivals of COVID-19 patients and emergency patients by controlling the admission of elective patients and retrofitting beds, which can help improve bed utilization and overall patient survival.
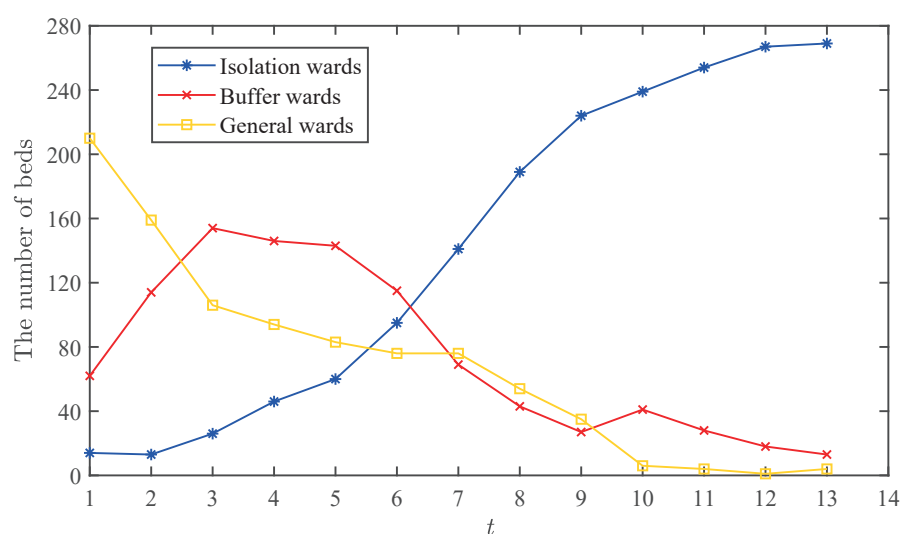

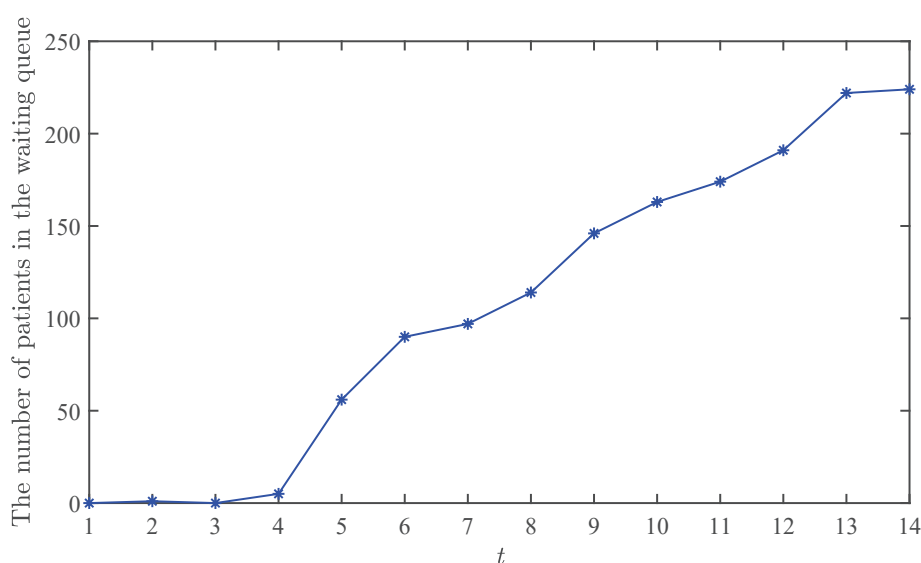**Figure 4.** The number of beds in different types of wards.

Figure 5. The number of patients in the waiting queue in base case.

6.3. Sensitivity Analysis

In this section, a sensitivity analysis is used to verify the effectiveness of the proposed model in dealing with different situations. We first conduct the experiments with some variations in the total number of beds, the arrival rate of COVID-19 patients, and the arrival rate of elective patients to explore the impact of the pandemic outbreak on hospital operations. Then, we compare our optimal policy with some benchmarks. Note that all the other parameters we do not mention are the same as the baseline values.

6.3.1. Impact of the Total Number of Beds

We first consider the impact of the total number of beds by varying N from 206 to 366 with a difference of 40. Table 4 shows the execution time of the BBO-DBPA algorithm in seconds and the total operating cost depending on the number of beds. Moreover, we investigate the impact of the total number of beds on the optimal dynamic policy in Table 5. We can see that the trend of each decision variable is roughly the same as the base case when we change the total number of beds. The larger the number of beds, the larger the number of general beds retrofitted to buffer beds, the larger the number of buffer beds retrofitted to isolation beds, and the larger the number of elective patients admitted.

Table 4. The execution time and optimization results in case 1.

N	206	246	286	326	366
The execution time	1013	996	992	991	1004
The total operating cost	48,958	28,546	22,672	18,603	14,946

In the first periods, the number of general beds retrofitted to buffer beds and the number of elective patients admitted when $N = 206$ and 246 are smaller than those when $N = 286$, 326, and 366. The reason is that the empty beds are insufficient to retrofit from general wards to buffer wards. On days 9 to 14, the number of admitted elective patients when $N = 326$ and 366 is more than when $N = 206$, 246, and 286. The reason is that the supply of buffer beds when $N = 326$ and 366 is more abundant than when $N = 206$, 246, and 286, so more elective patients can be admitted.

Figures 6–9 show the number of beds in each type of ward and the number of patients in the waiting queue under the different total numbers of beds, respectively. In Figures 6–9, the blue, red, green, black, and mauve lines indicate the corresponding indicator values when the total number of beds is 206, 246, 286, 326, and 366, respectively. As the total number of beds increases, the number of beds in each type of ward increases, and the number of patients in the waiting queue decreases. The reason is that different types of beds are in short supply for admitting all patients requiring hospitalization. When $N = 326$ and 366, the number of patients in the waiting queue decreases from day 13 to 14. The reason is that there is a sufficient supply of buffer beds to allow elective patients to be admitted.
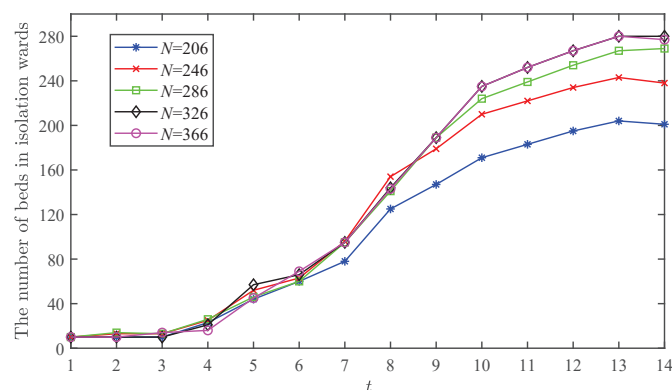

Figure 6. The number of beds in isolation wards in case 1.

Table 5. Comparison of optimal decision schemes in case 1.

Decision Variable	N	t = 1	t = 2	t = 3	t = 4	t = 5	t = 6	t = 7	t = 8	t = 9	t = 10	t = 11	t = 12	t = 13	t = 14
$n_{1,t}$	206	0	0	13	21	16	18	47	22	24	12	12	9	0	0
	246	3	0	12	27	11	33	58	25	31	12	12	9	0	0
	286	4	0	13	20	14	35	46	48	35	15	15	13	2	0
	326	0	0	11	36	9	29	49	45	46	17	15	13	0	0
	366	0	4	2	29	24	26	48	46	46	17	15	13	0	0
$n_{2,t}$	206	3	41	36	13	16	5	15	32	16	0	9	0	0	0
	246	27	57	36	20	5	5	12	34	19	1	10	0	0	1
	286	56	51	53	12	11	7	0	22	19	29	2	3	0	2
	326	58	50	61	45	11	0	0	13	19	22	17	3	0	0
	366	75	34	48	78	27	0	0	8	16	22	17	11	0	1
$n_{3,t}$	206	0	0	0	0	0	0	0	0	0	0	0	0	3	0
	246	0	0	0	0	0	0	0	0	0	0	0	0	5	0
	286	0	1	0	0	0	0	0	0	0	0	0	0	3	0
	326	0	0	0	0	0	0	0	0	0	0	0	0	0	5
	366	0	0	0	0	0	0	0	0	0	0	0	0	3	7
$n_{4,t}$	206	0	0	0	0	0	0	0	0	0	0	0	0	0	0
	246	0	0	0	0	0	0	0	0	0	0	0	0	1	0
	286	0	0	0	0	0	0	0	0	0	0	0	0	0	0
	326	0	0	0	0	0	0	0	0	0	0	0	0	2	0
	366	0	0	0	0	0	0	1	0	0	0	0	0	1	0
x_t	206	13	37	34	28	53	27	12	6	12	11	9	0	1	1
	246	34	54	34	27	25	22	12	6	12	11	10	0	3	4
	286	60	51	50	25	28	20	8	8	20	28	15	6	9	11
	326	61	50	55	54	30	19	1	9	25	34	27	20	27	33
	366	61	50	55	76	43	18	1	9	31	34	27	33	33	39
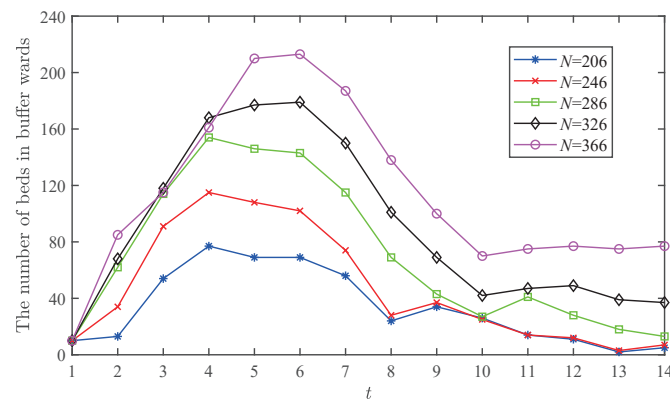
Figure 7. The number of beds in buffer wards in case 1.
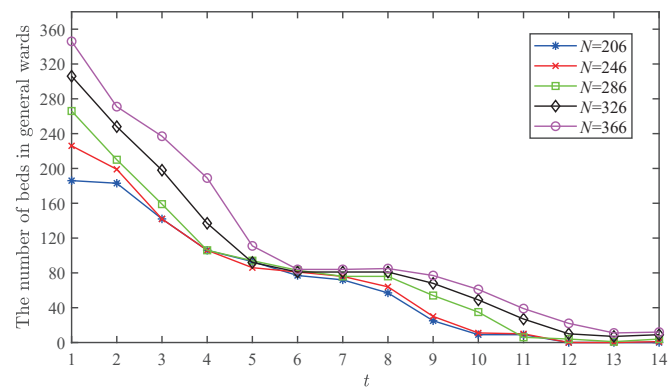
Figure 8. The number of beds in general wards in case 1.
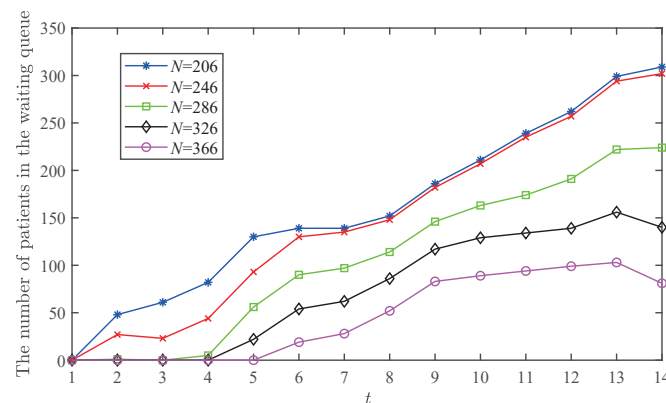
Figure 9. The number of patients in the waiting queue in case 1.

6.3.2. Impact of the Arrival Rate of COVID-19 Patients

We now consider the impact of the arrival rate of COVID-19 patients by varying $\lambda_{1,1,t}$ from 0.5 to 1.5 times the base case's value with a difference of 0.25. Table 6 shows the execution time of the BBO-DBPA algorithm in seconds and the total operating cost depending on the arrival rate of COVID-19 patients.

Table 6. The execution time and optimization results in case 2.

Multiple of Base Case's $\lambda_{1,1,t}$	0.5	0.75	1	1.25	1.5
The execution time	982	970	980	985	963
The total operating cost	8125	17982	26142	49188	79268

We investigate the impact of the arrival rate of COVID-19 patients on the optimal dynamic policy in Table 7. We can see that the trend of each decision variable is roughly the same as the base case when we change the arrival rate of COVID-19 patients. Moreover, the larger the arrival rate of COVID-19 patients, the larger the number of buffer beds retrofitted to isolation beds, and the smaller the number of elective patients admitted. It suggests that hospitals should admit fewer elective patients, thus freeing up beds to admit more new arriving COVID-19 patients to reduce the total operating cost.

Table 7. Comparison of optimal decision schemes in case 2.

Decision Variable	Multiple of Base Case's $\lambda_{1,1,t}$	$t = 1$	$t = 2$	$t = 3$	$t = 4$	$t = 5$	$t = 6$	$t = 7$	$t = 8$	$t = 9$	$t = 10$	$t = 11$	$t = 12$	$t = 13$	$t = 14$
$n_{1,t}$	0.5	4	0	0	8	10	22	27	25	27	14	9	0	0	0
	0.75	4	0	2	7	15	36	36	36	35	17	13	5	0	0
	1	4	0	3	16	19	45	45	48	38	17	13	10	0	0
	1.25	4	0	8	15	20	60	69	20	29	10	13	12	0	0
	1.5	4	0	2	22	25	58	64	20	25	11	14	12	0	0
$n_{2,t}$	0.5	57	51	54	47	3	0	0	0	9	21	7	1	0	4
	0.75	58	54	57	34	7	0	0	3	9	20	11	5	0	4
	1	58	54	61	32	6	1	0	18	18	7	6	4	0	0
	1.25	57	59	57	19	8	5	7	26	7	0	11	5	0	0
	1.5	58	53	62	24	9	0	5	25	7	2	11	5	0	0
$n_{3,t}$	0.5	0	0	0	0	0	0	0	0	0	0	0	2	2	9
	0.75	0	0	0	0	0	0	0	0	0	0	0	0	0	4
	1	0	0	0	0	0	0	0	0	0	0	0	0	2	0
	1.25	0	0	0	0	0	0	0	0	0	0	0	0	6	1
	1.5	0	0	0	0	0	0	0	0	0	0	0	0	5	0
$n_{4,t}$	0.5	0	0	0	0	0	0	0	0	0	0	0	0	1	0
	0.75	0	0	0	0	0	0	0	0	0	0	0	0	1	0
	1	0	0	0	0	0	0	0	0	0	0	0	0	0	0
	1.25	0	0	0	0	0	0	0	0	0	0	0	0	0	0
	1.5	0	0	0	0	0	0	0	0	0	0	0	0	0	0
x_t	0.5	60	49	55	45	43	26	13	26	37	37	40	32	36	38
	0.75	62	50	55	30	28	16	7	17	32	39	33	25	29	30
	1	62	50	49	19	19	10	9	11	16	17	12	6	6	5
	1.25	62	49	36	12	3	0	13	6	13	12	12	2	6	7
	1.5	62	50	38	10	2	0	13	6	13	12	12	2	6	5

Figures 10–13 show the number of beds in each type of ward and the number of patients in the waiting queue under different arrival rates of COVID-19 patients, respectively. In Figures 10–13, the blue, red, green, black, and mauve lines represent the corresponding indicator values when the number of COVID-19 patients ($\lambda_{1,1,t}$) is 0.5, 0.75, 1, 1.25, and 1.5 multiples of the value of $\lambda_{1,1,t}$ in the base case, respectively. As the arrival rate of COVID-19 patients increases, the number of beds in isolation wards increases, the number of beds in buffer wards increases, the number of beds in general wards remains roughly the same, and the number of patients in the waiting queue increases. The reason is that different types of beds are in short supply for receiving all patients requiring hospitalization.

The number of the three types of beds is almost the same from day 1 to 4. The reason is that the isolation beds are in adequate supply due to the small number of arriving COVID-19 patients, and the buffer beds are in short supply because of the large number of non-COVID-19 patients. Thus, the empty beds in the general wards are mainly retrofitted to buffer beds to serve non-COVID-19 patients. When the arrival rate of COVID-19 patients is at 1.25 and 1.5 times the base case, the number of beds in all three different types is almost the same from day 10 to day 14. The reason is that hospital beds are almost already occupied by many COVID-19 patients, so there are no beds available to retrofit into isolation beds.
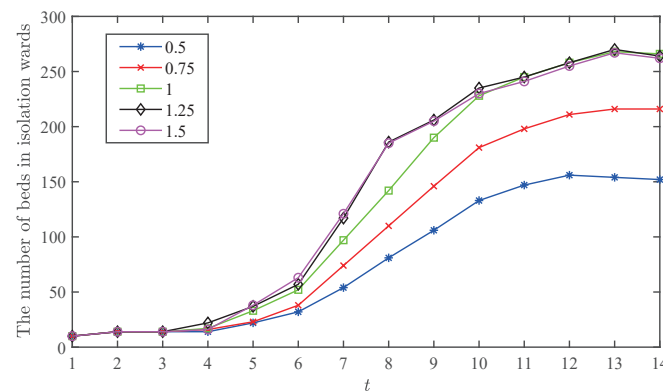

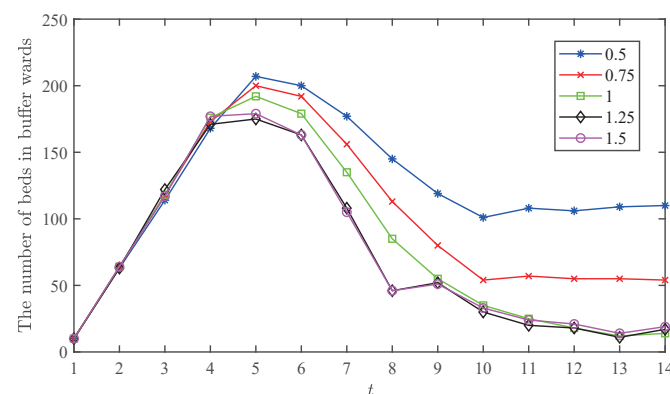**Figure 10.** The number of beds in isolation wards in case 2.

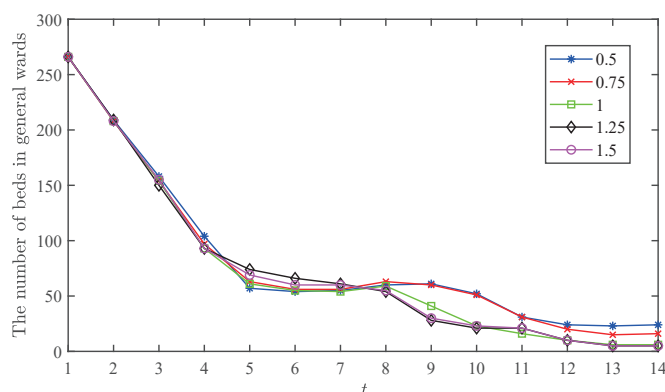**Figure 11.** The number of beds in buffer wards in case 2.

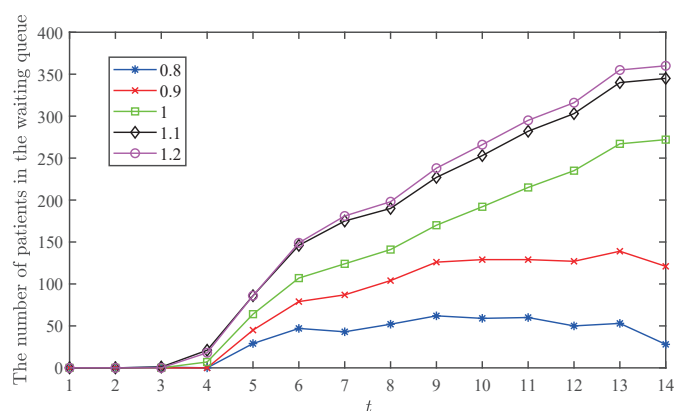**Figure 12.** The number of beds in general wards in case 2.

Figure 13. The number of patients in the waiting queue in case 2.

6.3.3. Impact of the Arrival Rate of Elective Patients

We now consider the impact of the arrival rate of elective patients by varying $\lambda_{3,2,t}$ from 0.8 to 1.2 times the base case's value with a difference of 0.1. Table 8 shows the execution time of the BBO-DBPA algorithm in seconds and the total operating cost depending on the arrival rate of elective patients.

Table 8. The execution time and optimization results in case 3.

Multiple of Base Case's $\lambda_{3,2,t}$	0.8	0.9	1	1.1	1.2
The execution time	972	980	965	975	973
The total operating cost	20,937	21,602	22,605	23,611	24,833

Furthermore, we investigate the impact of the arrival rate of elective patients on the optimal dynamic policy in Table 9. We can see that the trend of each decision variable is roughly the same as the base case when we change the arrival rate of elective patients. Moreover, the larger the arrival rate of elective patients, the larger the number of general beds retrofitted to buffer beds, and the larger the number of elective patients admitted. That is because the bigger the arrival rate of elective patients, the higher the demand for buffer beds.

Figures 14–17 show the number of beds in each type of ward and the number of patients in the waiting queue under different arrival rates of elective patients, respectively. In Figures 14–17, the blue, red, green, black, and mauve lines show the corresponding indicator values when the number of elective patients ($\lambda_{3,2,t}$) is 0.8, 0.9, 1, 1.1, and 1.2 multiples of the value of $\lambda_{3,2,t}$ in the base case, respectively. As the arrival rate of elective patients increases, the number of beds in isolation wards remains roughly the same, the number of beds in buffer wards increases, the number of beds in general wards decreases, and the number of patients in the waiting queue increases. This is because the bed demand for

COVID-19 patients has been met, and empty isolation beds are retrofitted to buffer beds to receive arriving elective patients.

Table 9. Comparison of optimal decision schemes in case 3.

| Decision Variable	Multiple of Base Case's $\lambda_{3,2,t}$	t = 1	t = 2	t = 3	t = 4	t = 5	t = 6	t = 7	t = 8	t = 9	t = 10	t = 11	t = 12	t = 13	t = 14
$n_{1,t}$	0.8	1	0	8	24	14	40	44	48	31	16	12	13	0	0
	0.9	2	0	12	22	15	34	46	48	31	17	13	13	0	0
	1	3	0	13	23	16	31	46	48	36	13	15	13	1	0
	1.1	5	0	14	25	12	29	46	48	39	12	15	13	0	0
	1.2	6	0	15	27	11	26	46	48	44	9	15	13	1	0
$n_{2,t}$	0.8	44	40	46	25	8	15	4	22	16	26	16	2	0	0
	0.9	49	47	52	17	13	4	2	22	17	29	7	6	0	2
	1	54	52	55	15	13	2	1	21	19	28	1	3	0	3
	1.1	62	58	46	18	9	3	0	22	21	19	5	1	0	3
	1.2	67	62	46	19	8	3	0	20	23	8	8	1	0	2
$n_{3,t}$	0.8	0	0	0	0	0	0	0	0	0	0	0	0	0	0
	0.9	0	0	0	0	0	0	0	0	0	0	0	0	1	1
	1	0	1	0	0	0	0	0	0	0	0	0	0	0	0
	1.1	0	0	0	0	0	0	0	0	0	0	0	0	0	0
	1.2	0	0	0	0	0	0	0	0	0	0	0	0	0	0
$n_{4,t}$	0.8	0	0	0	0	0	0	0	0	0	0	0	0	2	0
	0.9	0	0	0	0	0	0	0	0	0	0	0	0	5	0
	1	0	0	0	0	0	0	0	0	0	0	0	0	3	0
	1.1	0	0	0	0	0	0	0	0	0	0	0	0	3	0
	1.2	0	0	0	0	0	0	0	0	0	0	0	0	2	0
x_t	0.8	48	41	44	27	17	6	1	0	10	20	20	10	17	16
	0.9	53	47	49	27	23	11	4	4	14	22	21	9	14	18
	1	59	52	52	25	30	18	5	7	21	28	14	9	9	13
	1.1	66	56	45	32	37	27	9	8	24	30	12	8	9	12
	1.2	70	60	44	34	44	38	8	13	28	28	16	5	8	10
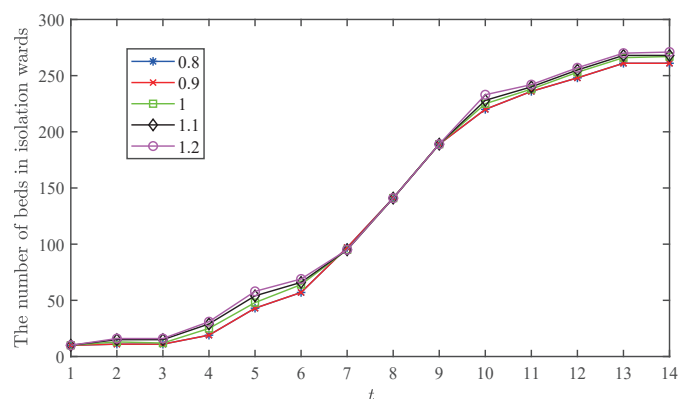
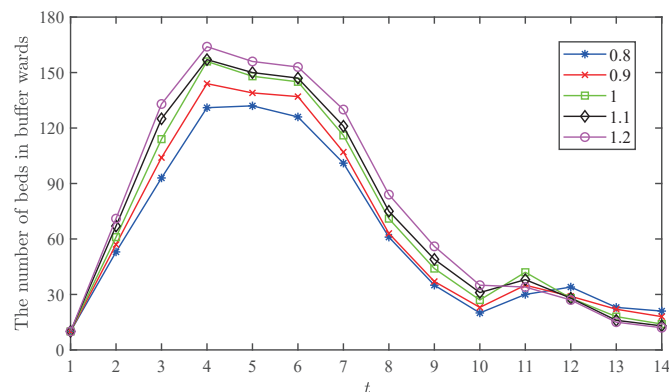**Figure 14.** The number of beds in isolation wards in case 3.

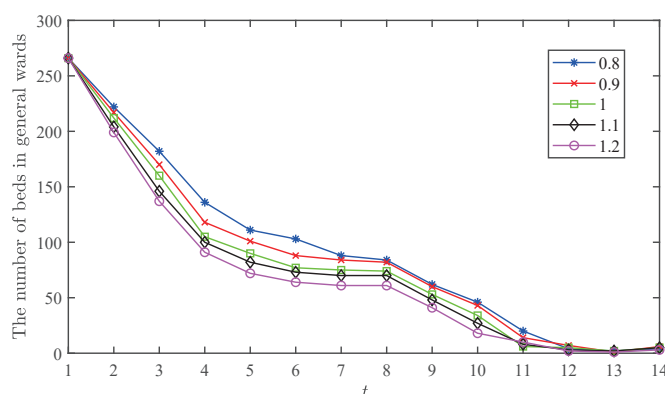**Figure 15.** The number of beds in buffer wards in case 3.

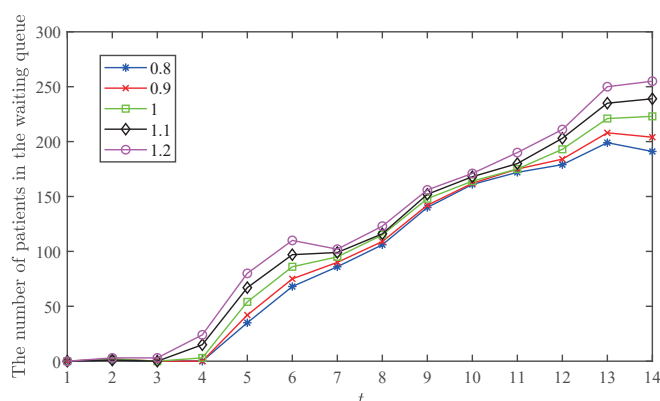**Figure 16.** The number of beds in general wards in case 3.

Figure 17. The number of patients in the waiting queue in case 3.

6.3.4. Performance Evaluation with Benchmark Policies

We explore the performance evaluation of the optimal dynamic policy by comparing it with some benchmark policies. Inspired by the different hospital operational management, we propose the following three benchmark policies from the perspective of bed retrofit policy and patient admission control policy: (1) only adopting bed retrofit policy (dynamic bed allocation), (2) only adopting patient admission control policy, and (3) neither adopting bed retrofit policy nor patient admission control policy. For simplicity, we denote the three benchmark policies above as BR policy, AC policy, and nBR–nAC policy, respectively. We define the optimal dynamic policy proposed in this paper (i.e., simultaneously adopting bed retrofit policy and patient admission control policy) as BR–AC policy.

These benchmark policies have data settings that are consistent with the base case to guarantee fairness. Obviously, some parameters are not available under a specific policy. Our objective is to measure the total operating cost in four different dynamic policies.

Figure 18 shows the total operating cost under the four different policies. We can see that the BR–AC policy and BR policy are always better than the AC policy and the nBR–nAC policy. The reason is that the surge of COVID-19 patients and those requiring observation leads to an elevated demand for isolation beds and buffer beds. Thus adopting the bed retrofit policy can significantly reduce the total rejection cost for COVID-19 patients and the total waiting cost for elective patients, thereby significantly reducing the total operating cost of the hospital.

It also shows that the BR–AC policy always performs better than the BR policy. The reason is that based on using the bed retrofit policy and adopting the patient admission control policy can delay some treatment of elective patients and reserve some empty beds for emergency and COVID-19 patients who arrive in the future through the bed retrofit policy. Intuitively, the difference in the total operating cost between the AC policy and the nBR–nAC policy is slight as the total number of beds increases.
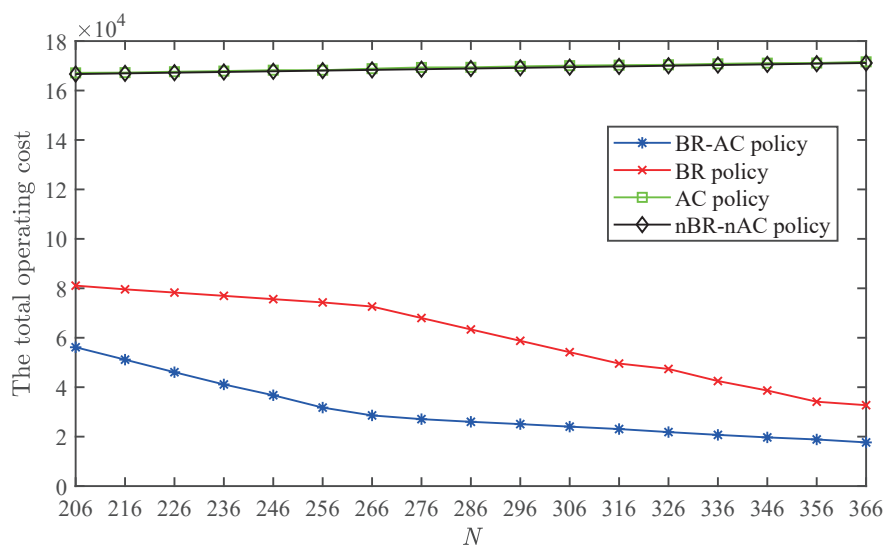
Figure 18. The total operating cost under four different policies.

We also find that the total operating cost under the AC policy and the nBR–nAC policy increase as N increases. In contrast, the total operating cost under the BR–AC policy and BR policy decreases as N increases. That is because our experimental setup is to add beds to the general wards. Thus the more general beds there are, the higher the empty cost the hospital has, thereby increasing the total operating cost. However, the BR–AC and BR policies can significantly reduce the total rejection cost for COVID-19 patients and the total waiting cost for elective patients. Moreover, the more general beds there are, the lower the hospital's total operating cost.

7. Conclusions and Future Research

We introduce a new problem of dynamic bed allocation and patient admission control for hospitals with three different types of wards and three kinds of patients during pandemics. In addition to isolation wards for COVID-19 patients and general wards for non-COVID-19 patients, we consider buffer wards for at-risk-of-COVID-19 patients to prevent nosocomial virus transmission further. To solve this problem, we formulate a MIP model to minimize the total operating cost of the hospital. By using the proposed BBO-DBPA algorithm, we find the approximate optimal solution. Through the analysis of numerical experiments, we discuss how the dynamic bed policy and patient admission control can effectively reduce the total operating cost of hospitals during the pandemic. In addition, we evaluate the performance of the optimal policy by comparing it with some benchmark policies. We conclude that when the admission control policy is used together with the dynamic bed policy, the total operating cost of the hospital is significantly reduced. Although our work is motivated by healthcare operations management under pandemics, our method and insights can also be applied to other service operations requiring screening and being assigned to different designated departments.

In future research, the proposed method could be extended to consider resource extension by adding additional medical staff and critical equipment or providing new suitable beds for hospitals and resource exchange among different hospitals. We can further study hospital resource allocation and patient admission control optimization by using the data-driven response to COVID-19. Note that intelligent medical care with the application of AI technology is an important direction for healthcare operations. Our future study will discuss the dynamic allocation of medical resources in hospitals with buffer wards based on machine learning technology.

Abbreviations

The following abbreviations are used in this manuscript:

COVID-19	Corona Virus Disease 2019
MIP	mixed-integer programming
BBO	biogeography-based optimization
BBO-DBPA	biogeography-based optimization for dynamic bed and patient admission

References

1. Yang, F.; Jiang, Y.; Tang, Z. Optimal admission control under premature discharge decisions for operational effectiveness. *Int. Trans. Oper. Res.* **2023**, *30*, 99–125. [CrossRef]
2. Huh, K.; Shin, H.S.; Peck, K.R. Emergent strategies for the next phase of COVID-19. *Infect. Chemother.* **2020**, *52*, 105. [CrossRef]
3. Shaheen, S.; Awwad, O.; Shokry, K.; Abdel-Hamid, M.; El-Etriby, A.; Hasan-Ali, H.; Shawky, I.; Magdy, A.; Nasr, G.; Kabil, H.; et al. Rapid guide to the management of cardiac patients during the COVID-19 pandemic in Egypt: "A position statement of the Egyptian Society of Cardiology". *Egypt. Heart J.* **2020**, *72*, 1–9.
4. Wee, L.E.; Conceicao, E.P.; Sim, X.Y.; Aung, M.K.; Tan, K.Y.; Wong, H.M.; Wijaya, L.; Tan, B.H.; Ling, M.L.; Venkatachalam, I. Minimizing intra-hospital transmission of COVID-19: The role of social distancing. *J. Hosp. Infect.* **2020**, *105*, 113–115. [CrossRef]
5. Asperges, E.; Novati, S.; Muzzi, A.; Biscarini, S.; Sciarra, M.; Lupi, M.; Sambo, M.; Gallazzi, I.; Peverini, M.; Lago, P.; et al. Rapid response to COVID-19 outbreak in Northern Italy: How to convert a classic infectious disease ward into a COVID-19 response centre. *J. Hosp. Infect.* **2020**, *105*, 477–479. [CrossRef]
6. Wee, L.E.I.; Sim, X.Y.J.; Conceicao, E.P.; Aung, M.K.; Tan, K.Y.; Ko, K.K.K.; Wong, H.M.; Wijaya, L.; Tan, B.H.; Venkatachalam, I.; et al. Containing COVID-19 outside the isolation ward: The impact of an infection control bundle on environmental contamination and transmission in a cohorted general ward. *Am. J. Infect. Control* **2020**, *48*, 1056–1061. [CrossRef] [PubMed]
7. He, H.; Jiarui, F.; Minghuan, G.; Ling, Y.; Shaohua, C.; Zhongxiang, C.; Xuan, S.; Yujia, C.; Hesheng, W.; Zongkui, M.; et al. Establishment and practice of "dual-triage and double-buffering" model in the management of COVID-19 in large comprehensive hospitals. *Chin. Hosp. Manag.* **2020**, *40*, 53–55. (In Chinese)
8. Wen, X.; Li, Y. Anesthesia procedure of emergency operation for patients with suspected or confirmed COVID-19. *Surg. Infect.* **2020**, *21*, 299. [CrossRef]
9. Heins, J.; Schoenfelder, J.; Heider, S.; Heller, A.R.; Brunner, J.O. A scalable forecasting framework to predict COVID-19 hospital bed occupancy. *INFORMS J. Appl. Anal.* **2022**, *52*, 508–523. [CrossRef]
10. Liu, M.; Cheng, S.Z.; Xu, K.W.; Yang, Y.; Zhu, Q.T.; Zhang, H.; Yang, D.Y.; Cheng, S.Y.; Xiao, H.; Wang, J.W.; et al. Use of personal protective equipment against coronavirus disease 2019 by healthcare professionals in Wuhan, China: Cross sectional study. *BMJ* **2020**, *369*, m2195. [CrossRef]
11. Hu, X.Y.; Yang, Q.X.; Xiao, C.Q.; Quan, L.L.; Chen, D.Y. Establishment and operation of buffer quarantine area in designated hospital during the pandemic of COVID-19. *Basic Clin. Med.* **2020**, *40*, 746. (In Chinese)
12. Hu, X.; Ma, X.; Hu, Y. Exploration and practice of setting up buffer wards in general hospitals in non-epidemic areas. *Chin. Hosp.* **2021**, *25*, 91–93.
13. Liu, R.; Xu, J.; Liu, Y. Dynamic patient admission control with time-varying and uncertain demands in Covid-19 pandemic. *IEEE Trans. Autom. Sci. Eng.* **2021**, *19*, 620–631. [CrossRef]
14. Pishnamazzadeh, M.; Sepehri, M.M.; Panahi, A.; Moodi, P. Reallocation of unoccupied beds among requesting wards. *J. Ambient. Intell. Humaniz. Comput.* **2021**, *12*, 1449–1469. [CrossRef]
15. Lei, X.; Na, L.; Xin, Y.; Fan, M. A mixed integer programming model for bed planning considering stochastic length of stay. In Proceedings of the 2014 IEEE International Conference on Automation Science and Engineering (CASE), New Taipei, Taiwan, 18–22 August 2014; pp. 1069–1074. [CrossRef]
16. Taramasco, C.; Olivares, R.; Munoz, R.; Soto, R.; Villar, M.; de Albuquerque, V.H. The patient bed assignment problem solved by autonomous bat algorithm. *Appl. Soft Comput.* **2012**, *81*, 105484. [CrossRef]

17. Bachouch, R.B.; Guinet, A.; Hajri-Gabouj, S. An integer linear model for hospital bed planning. *Int. J. Prod. Econ.* **2012**, *140*, 833–843. [CrossRef]

18. Wang, X.; Gong, X.; Geng, N.; Jiang, Z.; Zhou, L. Metamodel-based simulation optimization for bed allocation. *Int. J. Prod. Res.* **2020**, *58*, 6315–6335. [CrossRef]

19. Luo, L.; Li, J.; Xu, X.; Shen, W.; Xiao, L. A data-driven hybrid three-stage framework for hospital bed allocation: A case study in a large tertiary hospital in China. *Comput. Math. Methods Med.* **2019**, *2019*, 7370231. [CrossRef]

20. Zhou, L.; Geng, N.; Jiang, Z.; Wang, X. Multi-objective capacity allocation of hospital wards combining revenue and equity. *Omega* **2018**, *81*, 220–233. [CrossRef]

21. Sitepu, S.; Mawengkang, H.; Husein, I. Optimization model for capacity management and bed scheduling for hospital. *IOP Conf. Ser. Mater. Sci. Eng.* **2018**, *300*, 012016. [CrossRef]

22. Ma, X.; Zhao, X.; Guo, P. Cope with the COVID-19 pandemic: Dynamic bed allocation and patient subsidization in a public healthcare system. *Int. J. Prod. Econ.* **2022**, *243*, 108320. [CrossRef] [PubMed]

23. Demeester, P.; De Causmaecker, P.; Vanden Berghe, G. Applying a local search algorithm to automatically assign patients to beds. In Proceedings of the 22nd Conference on Quantitative Methods for Decision Making (ORBEL 22), Brussels, Belgium, 1–18 January 2008.

24. Demeester, P.; Souffriau, W.; De Causmaecker, P.; Berghe, G.V. A hybrid tabu search algorithm for automatically assigning patients to beds. *Artif. Intell. Med.* **2010**, *48*, 61–70. [CrossRef]

25. Bilgin, B.; Demeester, P.; Misir, M. One hyper-heuristic approach to two timetabling problems in health care. *J. Heuristics* **2012**, *18*, 401–434. [CrossRef]

26. Range, T.M.; Lusby, R.M.; Larsen, J. A column generation approach for solving the patient admission scheduling problem. *Eur. J. Oper. Res.* **2014**, *235*, 252–264. [CrossRef]

27. Hammouri, A.I.; Alrifai, B. Investigating biogeography based optimization for patient admission scheduling problems. *J. Theor. Appl. Inf. Technol.* **2014**, *70*, 413–421.

28. Hammouri, A.I. A modified biogeography-based optimization algorithm with guided bed selection mechanism for patient admission scheduling problems. *J. King Saud Univ.-Comput. Inf. Sci.* **2022**, *34*, 871–879. [CrossRef]

29. Turhan, A.M.; Bilgin, B. Mixed integer programming based heuristics for the patient admission scheduling problem. *Comput. Oper. Res.* **2017**, *80*, 38–49. [CrossRef]

30. Bastos, L.S.; Marchesi, J.F.; Hamacher, S.; Fleck, J.L. A mixed integer programming approach to the patient admission scheduling problem. *Eur. J. Oper. Res.* **2019**, *273*, 831–840. [CrossRef]

31. Ceschia, S.; Schaerf, A. Modeling and solving the dynamic patient admission scheduling problemunder uncertainty. *Artif. Intell. Med.* **2012**, *56*, 199–205. [CrossRef]

32. Bolaji, A.L.; Bamigbola, A.F.; Shola, P.B. Late acceptance hill climbing algorithm for solving patient admission scheduling problem. *Knowl.-Based Syst.* **2018**, *145*, 197–206. [CrossRef]

33. Zhu, Y.H.; Toffolo, T.A.; Vancroonenburg, W.; Berghe, G.V. Compatibility of short and long term objectives for dynamic patient admission scheduling. *Comput. Oper. Res.* **2019**, *104*, 98–112. [CrossRef]

34. Heydar, M.; O'Reilly, M.M.; Trainer, E.; Fackrell, M.; Taylor, P.G.; Tirdad, A. A stochastic model for the patient-bed assignment problem with random arrivals and departures. *Ann. Oper. Res.* **2022**, *315*, 813–845. [CrossRef]

35. Engl, T.; Harper, P.; Crosby, T.; Gartner, D.; Arruda, E.F.; Foley, K.; Williamson, I. Modelling lung cancer diagnostic pathways using discrete event simulation. *J. Simul.* **2021**, *2021*, 1–11. [CrossRef]

36. van den Broek d'Obrenan, A.; Ridder, A.; Roubos, D.; Stougie, L. Minimizing bed occupancy variance by scheduling patients under uncertainty. *Eur. J. Oper. Res.* **2020**, *286*, 336–349. [CrossRef]

37. Simon D. Biogeography-based optimization. *IEEE Trans. Evol. Comput.* **2008**, *12*, 702–713. [CrossRef]

38. Pollock, A.M.; Lancaster, J. Asymptomatic transmission of COVID-19. *BMJ* **2020**, *371*, m4851. [CrossRef]

39. Lauer, S.A.; Grantz, K.H.; Bi, Q.; Jones, F.K.; Zheng, Q.; Meredith, H.R.; Azman, A.S.; Reich, N.G.; Lessler, J. The incubation period of coronavirus disease 2019 (COVID-19) from publicly reported confirmed cases: Estimation and application. *Ann. Intern. Med.* **2020**, *172*, 577–582. [CrossRef]

40. Guan, W.J.; Ni, Z.Y.; Hu, Y.; Liang, W.H.; Ou, C.Q.; He, J.X.; Liu, L.; Shan, H.; Lei, C.L.; Hui, D.S. Clinical characteristics of coronavirus disease 2019 in China. *N. Engl. J. Med.* **2020**, *382*, 1708–1720. [CrossRef]

41. Zhao, S.; Musa, S.S.; Lin, Q.; Ran, J.; Yang, G.; Wang, W.; Lou, Y.; Yang, L.; Gao, D.; He, D.; et al. Estimating the unreported number of novel coronavirus (2019-nCoV) cases in China in the first half of January 2020: A data-driven modelling analysis of the early outbreak. *J. Clin. Med.* **2020**, *9*, 388. [CrossRef]